# Hydrogen-bond dynamics of water confined in cyclodextrin nanosponges hydrogel

**V. Crupi · A. Fontana · D. Majolino · A. Mele · L. Melone · C. Punta · B. Rossi · F. Rossi · F. Trotta · V. Venuti**

Received: 14 November 2013 / Accepted: 28 January 2014 / Published online: 6 February 2014

V. Crupi · D. Majolino · V. Venuti
Department of Physics and Earth Science,
University of Messina, Viale Ferdinando Stagno D'Alcontres 31,
98166 Messina, Italy

A. Fontana · B. Rossi · F. Rossi
Department of Physics, University of Trento, Via Sommarive 14,
38123 Povo, Trento, Italy

A. Mele · L. Melone · C. Punta
Department of Chemistry, Materials and Chemical Engineering
"G. Natta", Politecnico di Milano, Piazza L. Da Vinci 32,
20133 Milan, Italy

A. Mele · L. Melone · C. Punta
INSTM Local Unit, Politecnico di Milano, Milan, Italy

B. Rossi (✉)
INSTM Local Unit, University of Trento, Trento, Italy
e-mail: rossi@science.unitn.it

F. Trotta
Department of Chemistry, University of Torino,
Via Pietro Giuria 7, 10125 Turin, Italy

## Introduction

Cyclodextrin nanosponges (CDNS) are cross-linked polymers made up of cyclodextrins (CD) showing intriguing properties [1]. The reaction of polycondensation between CD and suitable cross linking agents leads to the formation of CDNS, a 3-dimensional sponge-like structure showing both hydrophilic and hydrophobic nano-sized cavities. Cyclodextrin nanosponges are safe and biodegradable material with negligible toxicity on cell cultures, as recently shown by preliminary toxicity studies [2]. They are considered to exhibit superior inclusion ability with respect to native CD [1] by incorporating a large class of molecules within their structure, either as inclusion com-plexes or as non-inclusion adducts [3–8]. Thanks to these properties and their versatile structure, CDNS are recently proposed as efficient nano-sized delivery system suitable

for a broad range of applications in different technological fields [9–17].

Generally speaking, nanosponges are hyper-cross-linked cyclodextrins obtainable by polycondensation between α-, β- or γ-CD and suitable cross-linking agents, such as carbonyldiimidazole (CDI) [18–20], pyromellitic anhydride (PMA) [18, 21, 22] or activated derivatives of ethylenediaminetetraacetic acid (EDTA) [23]. Recent studies based on inelastic light scattering experiments [18, 19, 21–23], nuclear magnetic resonance and infrared spectroscopy measurements [19, 20, 22, 23] and numerical computations [19, 22] clearly evidenced that the cross-linking degree and the elastic properties of CDNS can be successfully modulated by varying the chemical structure of the cross-linking agent and by acting on the relative amount of the cross-linker with respect to the monomer CD (i.e. n = cross-linking agent molar excess with respect to CD) during the synthetic procedure.

Many types of CDNS exhibit a marked swelling behaviour in the presence of aqueous solution, leading to the formation of highly viscous, gel-like dispersion, similarly to hydrogel [21, 24–26]. This ability to absorb a large amount of water shown by some of CDNS is intriguing in view of their possible use as efficient water nano-containers. Additionally, CDNS hydrogel have been used as chiral reaction environment for photochemical asymmetric synthesis with noticeable capability of asymmetric induction [26]. Finally, the transition from rigid gel to a liquid suspension of selected CDNS was recently reported by gradual increase of the hydration level of CDNS [26, 27].

The inspection of the vibrational dynamics of CDNS hydrogel, performed over different frequency regimes by using Infrared and Raman spectroscopy [24, 25, 27], suggested that the swelling phenomena of CDNS involves both non-covalent physical interactions and covalent bonds. More specifically, the water holding capacity of the hydrogel and the specific phase exhibited by the system, i.e. rigid gel network or liquid suspension, are strictly connected to the complex interplay of these chemical and physical interactions over different length-scales [25, 27].

The hydration state and dynamics of cyclodextrins in aqueous solution play a crucial role in controlling the structural and functional properties of these molecules [28]. In the specific case of the hydrogel obtained by swelling in aqueous solution of CDNS, the hydrogen-bond (HB) networks established among water molecules confined in the nano-sized pores of nanosponges are expected to have a crucial role in determining the rigidity of the hydrogel network and their maximum water holding capacity [24, 25, 27].

In this paper, the changes observed in the spectral shape of the OH stretching band of ester-bridged CDNS based on pyromellitic anhydride are explored as a function of the hydration level of the system. As well known [29–31], this vibrational band is particularly sensitive to the HB arrangements with different connectivity degrees in which the water molecules confined in nanoscopic media are involved.

The main purpose is to understand the microscopic origin of the sol-to-gel evolution exhibited by nanosponges hydrogel as increasing the water content with respect to polymer by observing the hydrogen-bonds dynamics of the water molecules entrapped in the pores of polymer matrix.

These results are beneficial in designing new cyclodextrin-based hydrogel with more efficient and versatile inclusion/release properties.

## Experimental methods

### Chemicals

The β-CDPMA14 nanosponge was obtained following a synthetic procedure previously reported [32–34]. In order to obtain the polymer, anhydrous β-CD was dissolved at room temperature in anhydrous DMSO containing anhydrous $Et_3N$. Then, the cross-linking agent pyromellitic anhydride (PMA) was added at molecular ratios of 1:4 under intense magnetic stirring. The polymerization was complete in few minutes obtaining a solid that was broken up with a spatula and washed with acetone in a Soxhlet apparatus for 24 h. The pale yellow solid was finally dried under vacuum.

The corresponding hydrogel of nanosponge was prepared by adding the dry samples of β-CDPMA14 of suitable amount of double-distilled water (Sigma) in order to obtain different levels of hydration $h$ in the range 3–25. The hydration level $h$ is defined as weight ratio $H_2O$/β-CDEDTA14. All the gel samples of hydrogels were freshly prepared and used for Raman scattering measurements.

### Raman spectroscopy

Vertically polarized and crossed Raman spectra ($I_{VV}$ and $I_{HV}$, respectively) were acquired at room temperature on nanosponges hydrogel directly prepared into an optical quartz cell of inner diameter 10 mm. Single mode exciting radiation at 647.1 nm (typical power of ≈100 mW) vertically polarized with respect to the scattering plane was provided by a Coherent–Innova Kr + laser. The light scattered in normal direction with respect to the incidence beam was analysed in the 2,600–3,900 $cm^{-1}$ energy range using a Jobin–Yvon U1000 double monochromator having a focal length of 1,000 mm and equipped with oholographic gratings of 1,800 grooves/mm.

The relative amplitude of the luminescence background observed in the Raman spectra in the 2,600–3,900 $cm^{-1}$

spectral range was less then a few percent in the gels examined. Therefore, the experimental profiles were corrected for the luminescence background by subtracting an interpolating baseline modelled as a linear function.

The deconvolution procedure of the OH stretching band was undertaken using second derivative computations for evaluating the wavenumbers of the maxima of the different sub-bands. Multiple curve fitting was then applied to the experimental profiles based on these wavenumber values, by using the routine provided in the PeakFit 4.0 software package. The strategy adopted was to use well-defined shape components of Gaussian functions with all the parameters allowed to vary upon iteration until converging "best-fit" solution is reached. The procedure adopted makes use of the minimum number of parameters. The "best-fit" is characterized by $r^2 \approx 0.9999$ for all the investigated systems.

## Results and discussion

In Fig. 1a, b the polarized and depolarized OH stretching profiles of some β-CDPMA14 hydrogel obtained at different hydration level *h* are reported. For a better comparison of the data the spectra have been normalized to the total area (integrated in the 2,800–3,800 $cm^{-1}$ range). In both the VV and HV spectra of Fig. 1a, b the characteristic OH stretching band of water [30, 31] can be recognized, along with the more narrow Raman peaks found between 2,850 and 3,050 $cm^{-1}$ and assigned to the vibrational modes of CH and $CH_2$ groups of cyclodextrin nanosponges [20].

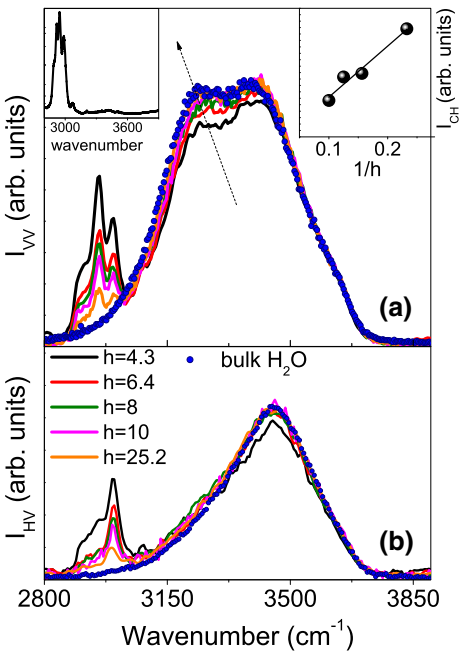


**Fig. 1** Polarized VV (**a**) and depolarized HV (**b**) Raman intensities of cyclodextrin nanosponges hydrogel al different level of hydration *h* in the OH stretching region. Polarized and depolarized profiles of neat water (*blue points*) are reported for comparison. Inset at the left: VV Raman profile of dry β-CDPMA14 nanosponge in the wavenumber range 2,800–3,900 $cm^{-1}$. *Inset at the right* Estimated intensity of vibrational modes assigned to CH vibrations of CDNS as a function of the mass ratio 1/h. (Color figure online)

The analysis of both the polarized and depolarized profiles acquired at different *h* values points out remarkable changes in the total intensity of the CH modes of CDNS when the content of nanosponge increases with respect to the water. In particular, the estimated total intensity $I_{CH}$ of the modes falling between 2,850 and 3,050 $cm^{-1}$ linearly rescales with the mass ratio 1/*h*, as shown for $I_{VV}$ profiles in the inset at the right of Fig. 1a. The same behaviour is found for $I_{CH}$ estimated from the depolarized spectra.

The VV Raman profile of dry β-CDPMA14 nanosponge is reported, in the wavenumber range 2,800–3,900 $cm^{-1}$, in the inset at the left of Fig. 1. It appears evident that the spectral contribution to the OH stretching band due to the OH groups of nanosponge is negligible compared to the signal arising from water. On the basis of this observation, we are confident that no subtraction procedure of the OH stretching signal of dry CDNS from the spectral profile of hydrated nanosponges is needed.

By focusing on the OH stretching band of water, remarkable changes in the spectral shape of this band can be observed in the polarized spectra of CDNS hydrogel by varying the hydration level, as indicated by the arrows in Fig. 1a. This finding suggests a great sensitivity of this spectral region to the structural modifications of the HB networks in which the water molecules are arranged in the hydrogel. As a general trend, it can be observed that an increase of the hydration level leads to the enhancement of the low-frequency contribution of the OH stretching band of polarized Raman intensity, thus suggesting an enhanced co-operativity in the H-bonds of water.

The same sensitivity can not be envisaged on the analysis of OH stretching band observed in the depolarized spectra $I_{HV}$ of hydrogel, since coupling among OH oscillators generally results in a strongly polarized contribution. As evidenced in Fig. 1b, the depolarized OH spectra exhibit only minor variations with respect to neat water reported in the same graph and, moreover, these variations are almost coincident for the different explored hydration levels of the system.

By following a well assessed model [35], the spectral variations, in shape and/or centre-frequency, observed for the polarized OH stretching profile can be related to different co-operativity degrees of the hydrogen-bond arrangements involving the water molecules attached to, or confined into, the pores of the CDNS. Taking these consideration into account, a full quantitative analysis of the spectral changes observed in the OH stretching band is then

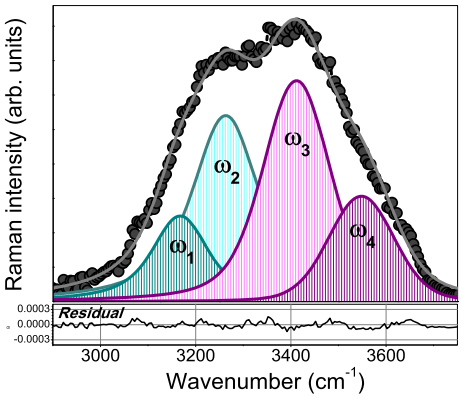


**Fig. 2** Typical schematic of the fitting procedure results for nanosponges hydrogel at $h = 4.3$

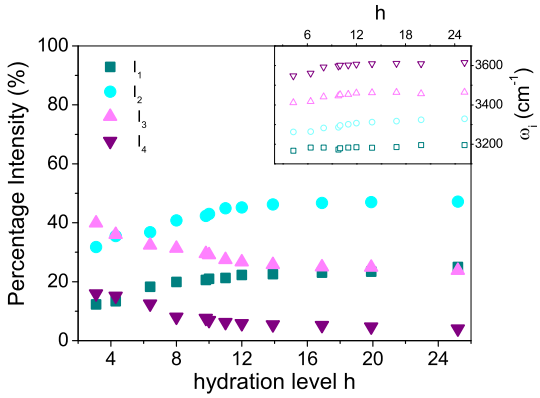


**Fig. 3** Percentage intensities $I_i$ of the different spectral contributions to the OH stretching band as a function of the hydration level $h$ for β-CDPMA14 hydrogel. Inset: evolution of the corresponding peak wavenumbers: $\omega_1$ *open squares*, $\omega_2$ *open circles*, $\omega_3$ *open up triangles*, $\omega_4$ *open down triangles*

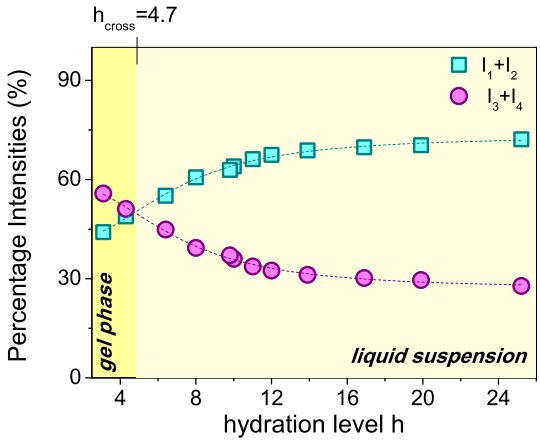


**Fig. 4** Percentage intensities $I_1 + I_2$ and $I_3 + I_4$ of the spectral contributions to the OH stretching band as a function of the hydration level $h$ for β-CDPMA14 hydrogel. The *vertical line* indicates the value estimated for $h_{cross}$

carried out by the deconvolution procedure already described in literature [36, 37].

Generally speaking, the assignments and interpretation of the spectral components of the broad OH band were reported in literature in different ways [38, 39]. However, there is substantial agreement that OH groups with a higher degree of HB order show a band at lower wavenumbers.

After a preliminary subtraction from the total experimental profile $I_{VV}$ of the spectral signal assigned to the CH vibrational modes of nanosponges, the polarized OH stretching band of water are decomposed into four different spectral components corresponding to four classes of OH oscillators (Fig. 2).

The two sub-bands at the lowest wavenumbers, namely $\omega_1$ and $\omega_2$, are assigned to the symmetric and asymmetric OH stretching modes of water molecules arranged in tetrahedral HB networks and, therefore, exhibiting strong hydrogen bonding on both the hydrogen atoms. The spectral component $\omega_3$ reflects the non-in-phase OH stretching mode of $H_2O$ molecules involved in distorted tetrahedral structures, commonly referred to as 'bifurcated H-bonds'. Finally, the highest wavenumber sub-band $\omega_4$ is representative of the OH mode of water molecules whose H-bond network is, totally or at least partially, broken.

Figure 2 displays a typical best fit result obtained for OH stretching profile of nanosponge hydrogel at h = 4.3 with the distinct spectral components highlighted.

It should be pointed out that the data analysis here proposed is carried out with the aim of a better quantification of the spectral-shape changes observed for the OH stretching band of water different hydrogel which are already qualitatively described above.

Figure 3 displays the evolution of the estimated percentage intensities $I_i$ (i = 1–4) of the different spectral contributions representative of the population of each class of OH oscillators as a function of the hydration $h$. In the inset, the behavior of the wavenumbers $\omega_i$ of each sub-band is reported as a function of the same parameter $h$.

A general slight increasing (about 2 %) of the values of center-frequencies $\omega_i$ is found for each spectral component, in agreement with the blue-shift of the broad distributions observed by inspection of raw experimental profiles of Fig. 1a. This finding suggests a general hardening of HB interactions involving the confined water molecules by increasing the hydration level of the hydrogel.

From the inspection of the evolution of intensities $I_i$ reported in Fig. 3, it clearly appears that an increase of the hydration $h$ corresponds to an enhancement of the population of water molecules arranged in tetrahedral HB networks ($I_1$, $I_2$), i.e. bulk-like contribution. Correspondingly, a decreasing of the population of water molecules involved in HB network with connectivity less than four ($I_3$, $I_4$) is found when the hydration level increases in the system. These last contributions, namely not bulk-like contributions, are typically associated to water molecules

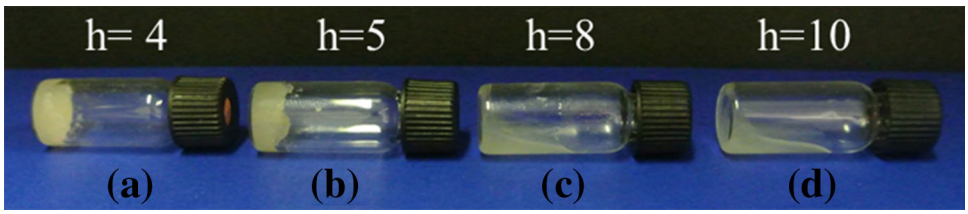


**Fig. 5** Photographs of the gel phase (**a**, **b**) and liquid suspension (**c**, **d**) observed for β-CDPMA14 hydrogel at level of hydration $h$ lower and higher than $h_{cross}$

"perturbed" by the presence of solutes or attached to some interface.

It is noteworthy that a characteristic saturation effect is observed at the high values of $h$ for all the populations $I_i$.

By starting from the findings of Fig. 3, a more synthetic picture of the phenomena is pointed out in Fig. 4 where the sums of the intensities ($I_1 + I_2$) and ($I_3 + I_4$) are plotted as a function of $h$.

As a matter of fact, these quantities are representative of the population of the two different classes of water molecules, i.e. bulk-like (tetra-coordinated) and not bulk-like water molecules, respectively, found in the hydrogel system.

The $h$-dependence of the intensities data reported in Fig. 4 is well reproduced by using a logistic function (dashed curves in Fig. 4), consistently with the saturation behavior observed at high values of $h$ for both bulk-like and not bulk-like contributions.

More interestingly, Fig. 4 clearly gives evidence of the existence of a characteristic crossover point where the population of bulk-like water molecules becomes favored with respect to the population of not bulk-like water. The crossing point of the curves reported in Fig. 4 provides directly the hydration level at the cross-over conditions: $h_{cross} = 4.7$.

This experimental finding can be interpreted by considering saturation of the sites of water confinement of nanosponges observed for values of hydration level higher than the cross-over hydration $h_{cross}$. Indeed, above $h_{cross}$ the pores of CDNS are not able to adsorb additional water molecules. Consequently, at higher water content, $H_2O$ molecules tend to rearrange in more cooperative, bulk-like networks, due to the lack of available space inside the pores of the CDNS polymeric matrix.

The value of $h_{cross}$ defines two regions of concentration of nanosponges in water corresponding to different macroscopic phases exhibited from the system, as revealed in the photographs of Fig. 5. At low content of water with respect to CDNS polymer, i.e. $h < h_{cross}$, the swelling of nanosponges gives rise to a rigid opaque gel (the sample does not flow if turned upside down). By increasing the hydration levels, the initially rigid gel of β-CDPMA14 progressively tends to flow up to become a fluid suspension for $h > h_{cross}$.

The direct correspondence between the cross-over hydration level and the gel-to-sol phase transition observed for β-CDPMA14 hydrogel is consistent with the results achieved on another class of nanosponges hydrogel, obtained by using EDTA as cross-linking agent [27]. All these experimental results suggest that the cross-over point, i.e. the critical concentration of gelation of nanosponges, strongly depends both on the molecular structure of cross-liking agent used for obtaining the CDNS polymers and on the molar ratio $n$ [27]. In particular, if $n$ is kept fixed at $n = 4$, different concentrations of gelation are found on passing from PMA- to EDTA-nanosponges, as clearly evident by comparing the cross-over hydration levels estimated for the two different types of nanosponge-hydrogel (i.e., $h_{cross} = 17$ and 4.7 for β-CDEDTA14 [27] and β-CDPMA14, respectively). This means that the saturation of the confinement sites of water (i.e. the pores of the nanosponge) is reached at lower hydration levels for β-CDPMA14 hydrogel with respect to β-CDEDTA14. This finding strongly suggests the conclusion that β-CDPMA14 hydrogel exhibit significant lower swelling properties with respect to β-CDEDTA14, which appear to be the most absorbent polymer. These results appear to be particularly relevant for practical applications of these CD-based hydrogels and they are likely to be exploited for the design of suitable stimuli-responsive systems.

Finally, a further confirmation of the results discussed above is provided by using a different approach for describing the OH stretching contribution, as suggested by the model of Green, Lacey and Sceats (GLS) [29].

Theoretical studies [40] suggest that the low-frequency feature of the OH stretching band of water which appears in the polarized spectrum essentially arises from a collective in-phase stretching motions of the OH groups of water molecules. As a matter of fact, the shoulder at low frequency appears as a result of the large net polarizability change of these vibrational modes. GLS model proposes that this collective band arises from the collective in-phase stretching motion of the water molecules involved in the fully bonded tetrahedral HB network. Consistently with this suggestion, other studies on aqueous solutions have shown that the presence of perturbations which tend to break or distort HB patterns, reduces the intensity of collective band [29, 30].

The relative collective intensity, $I_C$, of the low-frequency shoulder in the $I_{VV}$ spectrum, ascribed to "collective" modes of the OH groups, is assumed to be characterised by a depolarisation ratio which differs from that of uncoupled

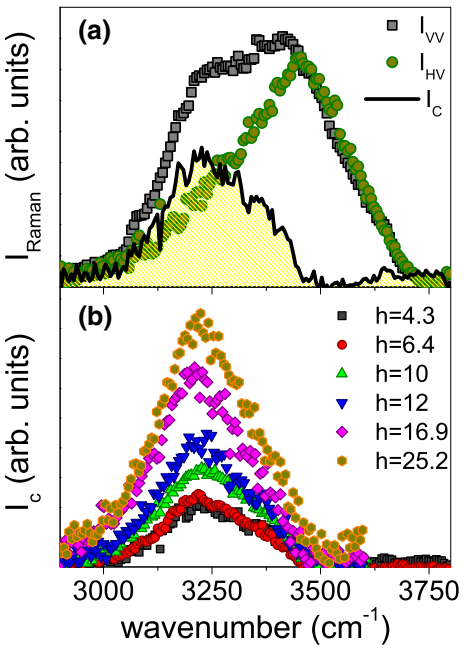


**Fig. 6** **a** Example of stripping procedure result for β-CDPMA14 hydrogel at $h = 4.3$. **b** Collective intensities Ic obtained for nanosponges hydrogel at different hydration levels $h$

OH oscillators (the remainder of the spectrum), whose depolarisation ratio $\rho_{OH}$ is relatively constant and approximately equal to that of an isolated OH oscillator. Hence, in order to obtain $I_C$, one can assume that the $I_{VH}$ spectrum is a scaled-down version of the $I_{VV}$ spectrum without the collective contribution. This suggest that $I_C$ can be, approximately, extracted by the difference spectrum $I_C(\omega) = I_{VV}(\omega) - aI_{VH}(\omega)$, where $a = [\rho_{OH}]^{-1}$.

Figure 6a displays the results of stripping procedure obtained for β-CDPMA14 hydrogel at $h = 4.3$, as an example.

The increasing of the collective intensities $I_C$ as a function of hydration level $h$, as shown in Fig. 6b, gives evidence of the corresponding growing of population of water molecules identified as bulk-like contributions, when the content of water increase with respect to CDNS polymer in the hydrogel. This finding is in full agreement with the conclusion achieved from the spectral deconvolution analysis, thus confirming the reliability of the experimental data handling.

## Conclusions

The hydrogen-bonds dynamics of water molecules confined in the nanoporous matrix of cyclodextrin nanosponges hydrogel is here investigated by using Raman scattering experiments. The analysis of the spectral shape of the characteristic OH stretching band of water observed in the high frequency range of the Raman spectra of PMA–CDNS hydrogel allowed us to distinguish among different HB patterns in which the confined water molecules are arranged.

The frequency and intensity evolution of these spectral components are monitored during the progressively increasing of the water content with respect to nanosponges in the hydrogel, following the transition of the polymers from a state of a rigid gel into a liquid suspension.

The spectral deconvolution analysis gives evidence of the existence of a characteristic cross-over hydration level above which the population of bulk-like water molecules becomes favored with respect to the not bulk-like contributions. The estimated value of $h_{cross}$ defines two regions of concentration of nanosponges in water which correspond to the different macroscopic phases exhibited from the system, i.e. rigid gel state and fluid suspension. Consistently, the observed cross-over has been associated to the rearrangement of water molecules in more cooperative, bulk-like networks as a consequence of saturation sites of water confinement of nanosponges found for hydration levels higher than $h_{cross}$.

The results of spectral deconvolution analysis are further confirmed by the inspection of the collective intensities estimated by following the GLS model.

These findings, in full agreement with the direct evidence of gel–sol transition in EDTA-nanosponges hydrogel recently revealed by Infrared spectroscopy measurements, further support the existence of a specific phase diagram of the cyclodextrin nanosponges hydrogel, where both the parameter $n$ and the molecular structure of the cross-linking agent play a fundamental role in defining the nano- and microscopic properties of the system.

**Acknowledgments** We thank Dr. Fabio Toraldo for his help.

## References

1. Trotta, F., Zanetti, M., Cavalli, R.: Cyclodextrin-based nanosponges as drug carriers. Beilstein J. Org. Chem. **8**, 2091–2099 (2012)
2. Cavalli, R., Donalisio, M., Bisazza, A., Civra, A., Ranucci, E., Ferruti, P., Lembo, D.: Enhanced antiviral activity of acyclovir loaded into nanoparticles. Methods Enzymol. **509**, 1–19 (2012)
3. Lembo, D., Swaminathan, S., Donalisio, M., Civra, A., Pastero, L., Aquilano, D., Vavia, P., Trotta, F., Cavalli, R.: Encapsulation of acyclovir in new carboxylated cyclodextrin-based nanosponges improves the agent's antiviral efficacy. Int. J. Pharm. **443**(1–2), 262–272 (2013)
4. Minelli, R., Cavalli, R., Ellis, L., Pettazzoni, P., Trotta, F., Ciamporcero, E., Barrera, G., Fantozzi, R., Dianzani, C., Pili, R.: Nanosponge-encapsulated camptothecin exerts anti-tumor activity in human prostate cancer cells. Eur. J. Pharm. Sci. **47**(4), 686–694 (2012)
5. Torne, S., Darandale, S., Vavia, P., Trotta, F., Cavalli, R.: Cyclodextrin-based nanosponges: effective nanocarrier for tamoxifen delivery. Pharm. Dev. Technol. **17**, 1–7 (2010)

6. Swaminathan, S., Pastero, L., Serpe, L., Trotta, F., Vavia, P., Aquilano, D., Trotta, M., Zara, G.P., Cavalli, R.: Cyclodextrin-based nanosponges encapsulating camptothecin: physicochemical characterization, stability and cytotoxicity. Eur. J. Pharm. Biopharm. **74**, 193–201 (2010)
7. Shende, P., Deshmukh, K., Trotta, F., Caldera, F.: Novel cyclodextrin nanosponges for delivery of calcium in hyperphosphatemia. Int. J. Pharm. **456**, 95–100 (2013)
8. Darandale, S.S., Vavia, P.R.: Cyclodextrin-based nanosponges of curcumin: formulation and physicochemical characterization. J. Incl. Phenom. Macrocycl. Chem. **75**, 315–322 (2013)
9. Trotta, F.: Cyclodextrin nanosponges and their applications. In: Bilensoy, E. (ed.) Cyclodextrins in pharmaceutics, cosmetics and biomedicine: current and future industrial applications, pp. 323–342. Wiley, Hoboken (2011)
10. Seglie, L., Martina, K., Devecchi, M., Roggero, C., Trotta, F., Scariot, V.: The effects of 1-MCP in cyclodextrin-based nanosponges to improve the vase life of Dianthus caryophyllus cut flowers. Postharvest Biol. Technol. **59**, 200–205 (2011)
11. Mamba, B.B., Krause, R.W., Malefetse, T.J., Gericke, G., Sithole, S.P.: Cyclodextrin nanosponges in the removal of organic matter to produce water for power generation. Water SA **34**, 657–660 (2008)
12. Arkas, M., Allabashi, R., Tsiourvas, D., Mattausch, E.M., Perfler, R.: Organic/inorganic hybrid filters based on dendritic and cyclodextrin "nanosponges" for the removal of organic pollutants from water. Environ. Sci. Technol. **40**, 2771–2777 (2006)
13. Liang, L., De-Pei, L., Chih-Chuan, L.: Optimizing the delivery systems of chimeric RNA·DNA oligonucleotides. Eur. J. Biochem. **269**, 5753–5758 (2002)
14. Shende, P.K., Trotta, F., Gaud, R.S., Deshmukh, K., Cavalli, R., Biasizzo, M.: Influence of different techniques on formulation and comparative characterization of inclusion complexes of ASA with β-cyclodextrin and inclusion complexes of ASA with PMDA cross-linked β-cyclodextrin nanosponges. J. Incl. Phenom. Macrocycl. Chem. **74**, 447–454 (2012)
15. Trotta, F., Cavalli, R., Martina, K., Biasizzo, M., Vitillo, J., Bordiga, S., Vavia, P., Ansari, J.: Cyclodextrin nanosponges as effective gas carriers. J. Incl. Phenom. Macrocycl. Chem. **71**, 189–194 (2011)
16. Memisoglu-Bilensoy, E., Vural, I., Bochot, A., Renoir, J.M., Duchene, D., Hincal, A.A.: Tamoxifen citrate loaded amphiphilic beta-cyclodextrin nanoparticles: in vitro characterization and cytotoxicity. J. Control. Release **104**, 489–496 (2005)
17. Cavalli, R., Akhter, A., Bisazza, A., Giustetto, P., Trotta, F., Vavia, P.: Nanosponge formulations as oxygen delivery systems. Int. J. Pharm. **402**, 254–257 (2010)
18. Rossi, B., Caponi, S., Castiglione, F., Corezzi, S., Fontana, A., Giarola, M., Mariotto, G., Mele, A., Petrillo, C., Trotta, F., Viliani, G.: Networking properties of cross-linked polymeric systems probed by inelastic light scattering experiments. J. Phys. Chem. B **116**(17), 5323–5327 (2012)
19. Castiglione, F., Crupi, V., Majolino, D., Mele, A., Rossi, B., Trotta, F., Venuti, V.: Inside new materials: an experimental-numerical vibrational study of cyclodextrins-based polymers. J. Phys. Chem. B **116**(43), 13133–13140 (2012)
20. Castiglione, F., Crupi, V., Majolino, D., Mele, A., Panzeri, W., Rossi, B., Trotta, F., Venuti, V.: Vibrational dynamics and hydrogen bond properties of β-CD nanosponges: a FTIR–ATR, Raman and solid-state NMR spectroscopic study. J. Incl. Phenom. Macrocycl. Chem. **75**(3), 247–254 (2013)
21. Mele, A., Castiglione, F., Malpezzi, L., Ganazzoli, F., Raffaini, G., Trotta, F., Rossi, B., Fontana, A.: HR MAS NMR, powder XRD and Raman spectroscopy study of inclusion phenomena in βCD nanosponges. J. Incl. Phenom. Macrocycl. Chem. **69**(3–4), 403–409 (2011)
22. Castiglione, F., Crupi, V., Majolino, D., Mele, A., Rossi, B., Trotta, F., Venuti, V.: Effect of cross-linking properties on the vibrational dynamics of cyclodextrin-based polymers: an experimental–numerical study. J. Phys. Chem. B **116**(27), 7952–7958 (2012)
23. Crupi, V., Fontana, A., Giarola, M., Majolino, D., Mariotto, G., Mele, A., Melone, L., Punta, C., Rossi, B., Trotta, F., Venuti, V.: Connection between the vibrational dynamics and the cross-linking properties in cyclodextrins-based polymers. J. Raman Spectrosc. **44**(10), 1457–1462 (2013)
24. Castiglione, F., Crupi, V., Majolino, D., Mele, A., Rossi, B., Trotta, F., Venuti, V.: Vibrational spectroscopy investigation of swelling phenomena in cyclodextrin nanosponges. J. Raman Spectrosc. **44**(10), 1463–1469 (2013)
25. Crupi, V., Majolino, D., Mele, A., Rossi, B., Trotta, F., Venuti, V.: Modelling the interplay between covalent and physical interactions in cyclodextrin-based hydrogel: effect of water confinement. Soft Matter **9**, 6457–6464 (2013)
26. Liang, W., Yang, C., Zhou, D., Haneoka, H., Nishijima, M., Fukuhara, G., Mori, T., Castiglione, F., Mele, A., Caldera, F., Trotta, F., Inoue, Y.: Phase-controlled supramolecular photochirogenesis in cyclodextrin nanosponges. Chem. Commun. **49**, 3510–3513 (2013)
27. Crupi, V., Majolino, D., Mele, A., Melone, L., Punta, C., Rossi, B., Toraldo, F., Trotta, F., Venuti, V.: Direct evidence of gel–sol transition in cyclodextrin-based hydrogel as revealed by FTIR–ATR spectroscopy. Soft Matter (2014). doi:10.1039/C3SM52354C
28. Rossi, B., Comez, L., Fioretto, D., Lupi, L., Caponi, S., Rossi, F.: Hydrogen bonding dynamics of cyclodextrin–water solutions by depolarized light scattering. J. Raman Spectrosc. **42**(6), 1479–1483 (2011)
29. Green, J.L., Lacey, A.R., Sceats, M.G.: Spectroscopic evidence for spatial correlations of hydrogen bonds in liquid water. J. Phys. Chem. **90**, 3959–3964 (1986)
30. Crupi, V., Magazù, S., Majolino, D., Maisano, G., Migliardo, P.: Dynamical response and H-bond effects in confined liquid water. J. Mol. Liq. **80**, 133–147 (1999)
31. Crupi, V., Longo, F., Majolino, D., Venuti, V.: Raman spectroscopy: probing dynamics of water molecules confined in nanoporous silica glasses. Eur. Phys. J. Spec. Top. **141**, 61–64 (2007)
32. Trotta, F., Tumiatti, W.: Cross-linked polymers based on cyclodextrin for removing polluting agents. Patent WO 03/085002 (2003)
33. Trotta, F., Tumiatti, W., Cavalli, R., Zerbinati, O., Roggero, C.M., Vallero, R.: Ultrasound-assisted synthesis of cyclodextrin-based nanosponges. Patent number WO 06/002814 (2006)
34. Trotta, F., Tumiatti, W., Cavalli, R., Roggero, C., Mognetti, B., Berta, G.: Cyclodextrin-based nanosponges as a vehicle for antitumoral drugs. Patent number WO 09/003656 A1 (2009)
35. Goldman, N., Saykally, R.J.: Elucidating the role of many-body forces in liquid water. I. Simulations of water clusters on the VRT(ASP-W) potential surfaces. J. Chem. Phys. **120**, 4777–4789 (2004)
36. Giguère, P.A.: The bifurcated hydrogen-bond model of water and amorphous ice. J. Chem. Phys. **87**, 4835–4839 (1987)
37. Crupi, V., Interdonato, S., Longo, F., Majolino, D., Migliardo, P., Venuti, V.: A new insight on the hydrogen bonding structures of nanoconfined water: a Raman study. J. Raman Spectrosc. **39**, 244–249 (2008)
38. Freda, M., Piluso, A., Santucci, A., Sassi, P.: Transmittance Fourier transform infrared spectra of liquid water in the whole mid-infrared region: temperature dependence and structural analysis. Appl. Spectrosc. **59**, 1155–1159 (2006)
39. Schmidt, D.A., Miki, K.: Structural correlations in liquid water: a new interpretation of IR spectroscopy. J. Phys. Chem. A **111**, 10119–10122 (2007)
40. Sceats, M.G., Rice, S.A. In Franks, F. (ed) Water-A comprehensive treatise, vol. 7, chapter 2. Plenum Press, New York (1983)